

F2F, a model-independent method to determine the mass and width of a particle in the presence of interference

Li-Gang Xia

Department of Physics, Warwick University, CV4 7AL, UK

Abstract

It is generally believed that any particle to be discovered will have a TeV-order mass. Given its great mass, it must have a large decay width. Therefore, the interference effect will be very common if they and the Standard-Model (SM) particles contribute to the same final state. However, the interference effect could make a new particle show up not like a resonance, and it is difficult to search and measure its properties. In this work, a model-independent method, F2F (Fit To Fourier coefficients), is proposed to search for an unknown resonance and to determine its mass (M) and width (Γ) in the presence of interference. Basically it is to perform cosine Fourier transformation to the observable distributions in data and background. Then a function is fitted to the Fourier coefficients. The fitting function is based on the general propagator form, $1/(x^2 - M^2 + iM\Gamma)$. Thus it does not need any signal model. Toy experiments show that the obtained mass and width agree well with the inputs with a similar precision as using an explicit signal model.

I. INTRODUCTION

Many Beyond-Standard-Model (BSM) models predict heavy particles of the order of TeV. If we search with a final state to which the Standard-Model (SM) processes also contribute, some of the SM backgrounds will interfere coherently with the new signal. However, the interference effect could make things complicated. The new particle may appear as a bump, a dip or other strange structures (for experimental observation, see Ref. [1]; for experimental searches, see Ref. [2–5]; for phenomenologic analyses, see Ref. [6–8]) in the distribution of an observable. Therefore it is difficult to search for and measure the properties of the new particle if we have not yet had enough knowledge about the interaction mechanism. This is particularly difficult for the searches at hadron colliders like the Large Hadron Collider (LHC).

Let us consider a simplified interference model. Suppose x is an observable (like the invariance mass of the final particles), the differential cross section is

$$\frac{d\sigma}{dx} \propto \left| A_b(x) + \frac{k(x)e^{i\delta(x)}}{x^2 - M^2 + iM\Gamma} \right|^2 \quad (1)$$

Here A_b is the background amplitude (assuming it is real) and the other term, a Breit-Wigner (BW) resonance signal, describes a new particle with mass M and decay width Γ . $k(x)$ and $\delta(x)$ represent the strength and relative phase of the new amplitude. They could be functions of the observable. Without a good knowledge of the interaction mechanism, we cannot parameterize the interference effect well and thus cannot make statistic interpretation easily (in other words, we have to make many simulations and interpretate under many hypotheses) and measure the mass and width by fitting.

In this work, a novel method is proposed based on the fact that the squared propagator, $\frac{1}{(m^2 - M^2)^2 + M^2\Gamma^2}$, is the key factor for a resonance. The principle will be elaborated in next section. Toy experiments will be presented in Sec. III. We will summarize in Sec. IV.

II. PRINCIPLE OF THE METHOD

The differential cross section in Eq. 1 can be expanded to be a sum of three terms.

$$|A_b|^2 + \frac{k}{(x^2 - M^2)^2 + M^2\Gamma^2} + \frac{\sqrt{A_b k}((x^2 - M^2) \cos \delta + M\Gamma \sin \delta)}{(x^2 - M^2)^2 + M^2\Gamma^2} \quad (2)$$

The first term is the background process; the second term is the signal resonance and the third term is their interference. Let $f(x)/((x^2 - M^2)^2 + M^2\Gamma^2)$ denote the combination of the latter two terms. We will call it effective signal throughout this paper. Assuming $f(x)$ is a slow-varying function, the fast-varying component is mainly due to the factor $1/((x^2 - M^2)^2 + M^2\Gamma^2)$, namely, the mass and width. To measure the variation frequency, we can perform the Fourier transformation.

Supposing we have n measurements for an observable with the values x_1, x_2, \dots, x_n , the probability distribution function (normalized to the number of entries), $p(x)$, could be written either using a sum of Dirac delta functions or as a Fourier series.

$$p(x) = \sum_{i=1}^n \delta(x - x_i), \quad (3)$$

$$p(x) = c_0 + \sum_{k=1}^N c_k \cos \frac{k\pi(x - x_{\min})}{L} \quad (4)$$

where $L \equiv x_{\max} - x_{\min}$ and x_{\min}/x_{\max} is the smallest/greatest value. Now let us investigate how c_k s depend upon M and Γ through the squared propagator. With $\kappa \equiv k\pi/L$ and ignoring the slow-varying function $f(x)$, we have

$$c_k \propto \Re \int_{-\infty}^{+\infty} \frac{e^{i\kappa x}}{(x^2 - M_0^2)^2 + M_0^2\Gamma^2} dx, \quad (5)$$

where $M_0 \equiv M - x_{\min}$ (because the distribution is shifted by x_{\min} as shown in Eq. 4 so that it starts from 0 and ends at L). The integration can be done using the usual contour integration technique [9] and the result is

$$c_k \propto \frac{\pi}{\gamma_0^{3/2} \sin \theta} e^{-|\kappa| \sqrt{\gamma_0} \sin \frac{\theta}{2}} \cos(|\kappa| \sqrt{\gamma_0} \cos \frac{\theta}{2} - \frac{\theta}{2}). \quad (6)$$

Here $\gamma_0 \equiv \sqrt{M_0^2(M_0^2 + \Gamma^2)}$ and $\tan \theta \equiv \Gamma/M_0$. We can see that c_k as a function of k has two features. One is the exponential decay (mainly driven by non-vanishing Γ) and the other is the oscillation (mainly driven by non-vanishing M). In practise, we can fit the following function to the Fourier coefficients.

$$c_k(M, \Gamma, A, B, C) = A(x) + B e^{-|\kappa| \sqrt{\gamma_0} \sin \frac{\theta}{2}} \cos(|\kappa| \sqrt{\gamma_0} \cos \frac{\theta}{2} - C) \quad (7)$$

Here $A(x)$ is a polynomial function (second or third order is enough for toy experiments in next section) and B and C are two parameters. They are introduced to account for the slow-varying function not considered in the Fourier transformation.

On the other hand, we can calculate the coefficients easily for any sample according to the transformation law and the delta function form in Eq. 3.

$$c_0 = \frac{1}{L} \int p(x) dx = \frac{1}{L} \sum_{i=1}^n 1 = \frac{n}{L}, \quad (8)$$

$$c_k = \frac{2}{L} \int p(x) \cos \frac{k\pi(x - x_{\min})}{L} = \frac{2}{L} \sum_{i=1}^n \cos \frac{k\pi(x_i - x_{\min})}{L}. \quad (9)$$

To perform the fit, we need to know the uncertainty of c_k . Treating x_i ($i = 1, 2, \dots, n$) as n independent and identically-distributed (iid) random variables, c_k can be also seen as a random variable. Its variance can be obtained in the standard way, namely,

$$\sigma(c_k) = \frac{2}{L} \sqrt{\sum_i \left(\cos \frac{k\pi(x_i - x_{\min})}{L} - E\left[\cos \frac{k\pi(x - x_{\min})}{L} \right] \right)^2}, \quad (10)$$

where

$$E\left[\cos \frac{k\pi(x - x_{\min})}{L} \right] \equiv \frac{1}{n} \sum_i \cos \frac{k\pi(x_i - x_{\min})}{L} = \frac{L}{2n} c_k. \quad (11)$$

After obtaining the Fourier coefficients for the data and background, their subtraction gives the Fourier coefficients for the effective signal. Fitting the function in Eq. 7 to these coefficients will produce the best-estimated mass and width. Given the principle above, we will call the method F2F (Fit To Fourier coefficients).

In the derivation above, we have not yet considered the smearing effect because of imperfect detector response. If a function is expressed as a Fourier series, it is actually very convenient to take it into account.

$$\begin{aligned} p(x) &= \sum_k c_k \int_{-\infty}^{+\infty} \cos \frac{k\pi(y - x_{\min})}{L} \frac{1}{\sqrt{2\pi}\sigma} e^{-\frac{(x-y)^2}{2\sigma^2}} dy \\ &= \sum_k c_k e^{-\frac{1}{2}\left(\frac{k\pi\sigma}{L}\right)^2} \cos \frac{k\pi(x - x_{\min})}{L} \end{aligned} \quad (12)$$

The equation above shows that we need to add an extra exponential factor $e^{-\frac{1}{2}\left(\frac{k\pi\sigma}{L}\right)^2}$ for each Fourier coefficient. As a bonus, it also proves that unfolding is very difficult if we want to obtain the true distribution from the smeared distribution.

III. TOY EXPERIMENTS

In this section, let us investigate the performance of this method based on the following example. Suppose we have an exponential background and a Breit-Wigner resonance signal and they interfere coherently. The resonance has a mass, $M = 125$ GeV, and full width,

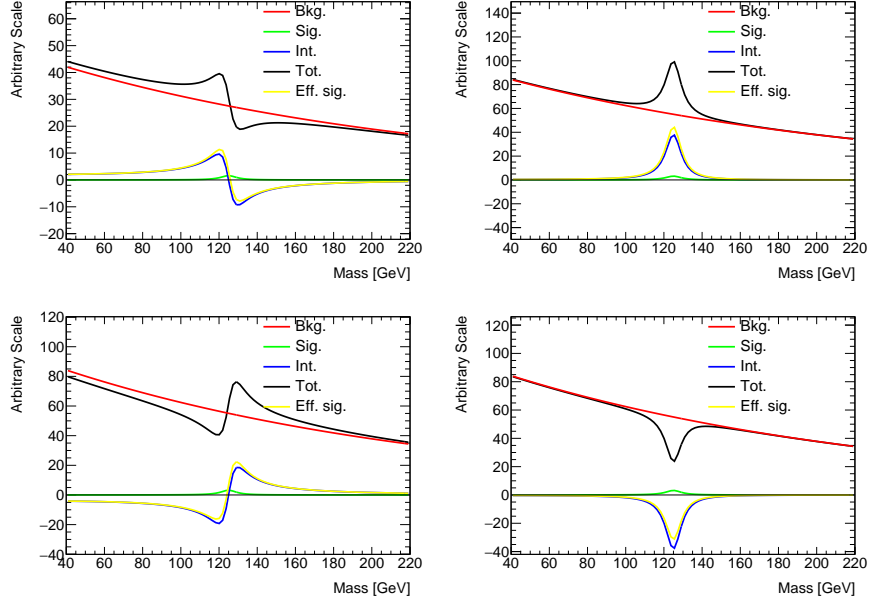


FIG. 1. (color online) Differential cross sections for different phase angles, $\delta = 180^\circ$ (top left), $\delta = 90^\circ$ (top right), $\delta = 0^\circ$ (bottom left) and $\delta = -90^\circ$ (bottom right). The red curve represents the background; green curve represents the signal; blue curve represents the interference contribution; black curve is the sum of all terms and the yellow curve represents the sum of signal and interference.

$\Gamma = 10$ GeV. To be exact, the differential cross section with respect to a mass variable is

$$\frac{d\sigma}{dx} \propto \left| \frac{\sqrt{b}}{\sqrt{\tau}} e^{-\frac{x}{2\tau}} + \frac{\sqrt{kbr} e^{i\delta}}{x^2 - M^2 + iM\Gamma} \right|^2, \quad (13)$$

where b represents the background yield; $k = \frac{2\sqrt{2}M\Gamma\gamma}{\pi\sqrt{M^2+\gamma}}$ with $\gamma \equiv \sqrt{M^2(M^2 + \Gamma^2)}$; $\tau = 200$ GeV is the decaying length for the background distribution; and $r = 0.005$ is the signal-to-background yield ratio. The mass distributions for 4 relative phases (180° , 90° , 0° and -90°) are shown in Fig. 1. We can see very different structures for the same particle.

A. Perfect detector resolution

In the first place, we do not consider the effect of the detector resolution. For each relative phase, a data sample, a background sample and a signal sample (the method itself does not need the signal sample) are produced. Figure 2 shows the fitting results using the explicit signal model, namely, the formula in Eq. 13. They will be compared with the method proposed in this work.

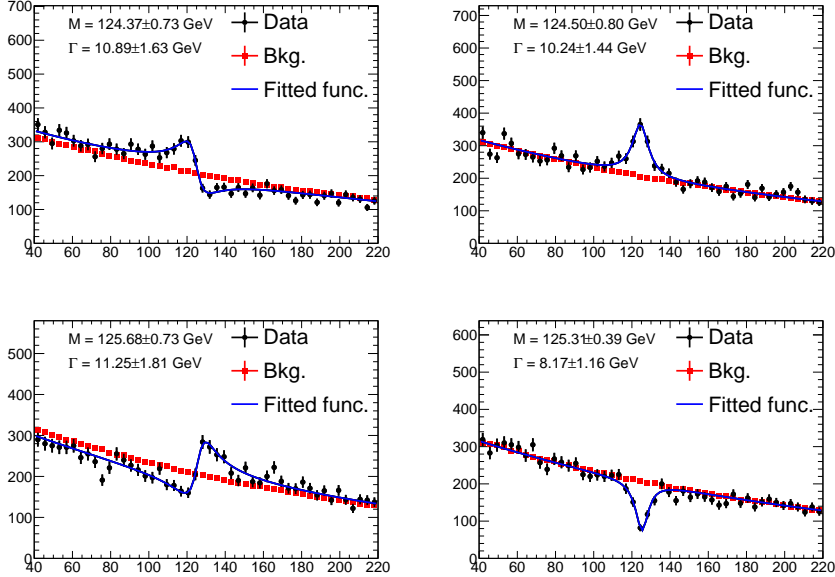


FIG. 2. (color online) Fitting results for different phase angles, $\delta = 180^\circ$ (top left), $\delta = 90^\circ$ (top right), $\delta = 0^\circ$ (bottom left) and $\delta = -90^\circ$ (bottom right). The black dots with error bar represent the data sample. The red squares represent the background sample. The blue curves represent the fit results.

For the purpose of validation, Fig. 3 shows the Fourier coefficients for a pure signal sample and also the fitting result using Eq. 7 in the F2F method. We can see the mass and width are well produced. In Eq. 3, the slow-varying contribution, namely the polynomial part in Eq. 7, is also shown. Throughout this section, we will use 30 terms in the Fourier series.

To use the F2F method, we do not need the signal sample, but calculate the Fourier coefficients for the data and background samples instead according to Eq. 9 and Eq. 10. The Fourier coefficients for the effective signal are obtained by their subtraction. Fitting Eq. 7 to these coefficients gives the final results. They are shown in Fig. 4. The results from the fits with an explicit signal model and the F2F method are summarized in Table I. They agree well with each other and also agree with the inputs. The precision using the F2F method is only worse a bit.

In the end of this section, it is worth making two comments. One is that we should not use the F2F method if we already have a good knowledge of the signal model or if there is no interference at all (then we can use bump-like functions to model the signal though the F2F method still applies in this case). The other is that we should not include the zero

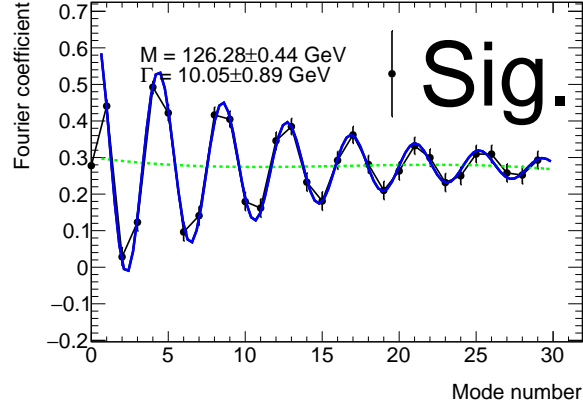


FIG. 3. (color online) Fitting results for a pure signal sample. The black dots with error bar represent the Fourier coefficients of the signal sample. The blue curves represent the full fitting results. The green dashed curves represents the slow-varying contribution, namely, the polynomial part in Eq. 7.

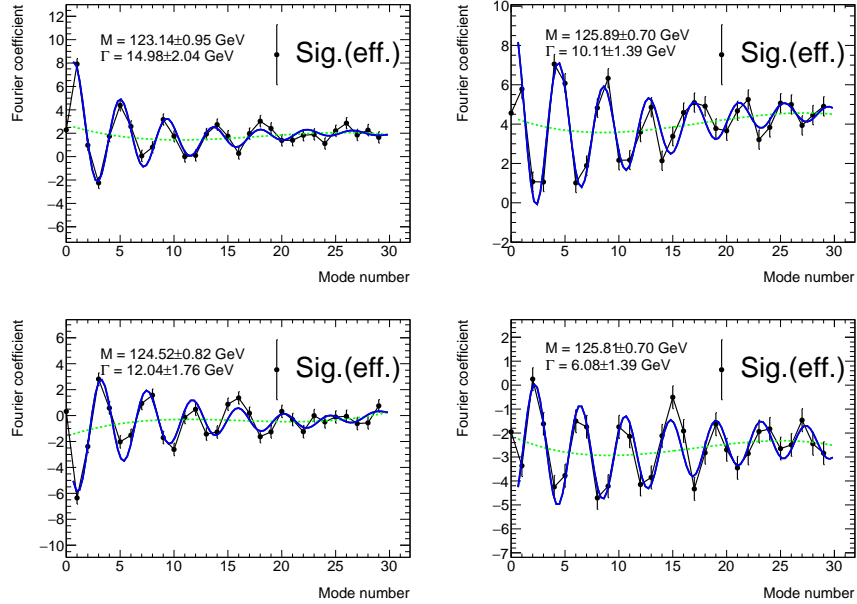


FIG. 4. (color online) Fitting results for different phase angles, $\delta = 180^\circ$ (top left), $\delta = 90^\circ$ (top right), $\delta = 0^\circ$ (bottom left) and $\delta = -90^\circ$ (bottom right). The black dots with error bar represent the Fourier coefficients of the effective signal (data subtracting background). The blue curves represent the full fitting results. The green dashed curves represents the slow-varying contribution, namely, the polynomial part in Eq. 7.

TABLE I. Summary of the fitting results on the mass and width in the case of perfect detector resolution.

Phase angle	Explicit signal model		F2F (this work)	
	Mass [GeV]	Width [GeV]	Mass [GeV]	Width [GeV]
180°	124.37 ± 0.73	10.89 ± 1.63	123.14 ± 0.95	14.98 ± 2.04
90°	124.50 ± 0.80	10.24 ± 1.44	125.89 ± 0.70	10.11 ± 1.39
0°	125.68 ± 0.73	11.25 ± 1.81	124.52 ± 0.82	12.04 ± 1.76
-90°	125.31 ± 0.39	8.17 ± 1.16	125.81 ± 0.71	6.08 ± 1.39

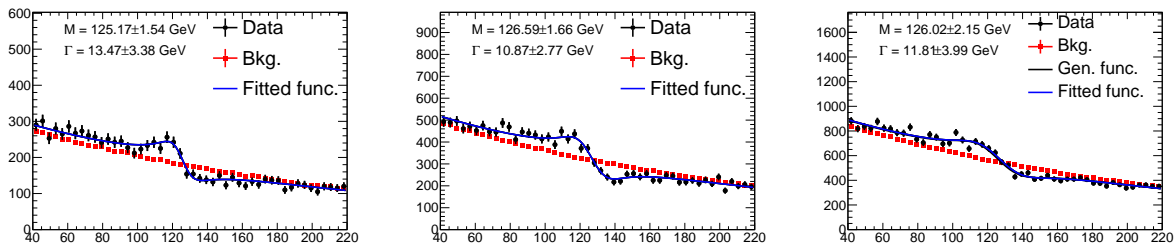


FIG. 5. (color online) Fitting results for three resolutions, 3 GeV (left), 6 GeV (middle) and 10 GeV (right). The black dots with error bar represent the data sample. The red squares represent the background sample. The blue curves represent the fit results.

mode in the fits for the F2F method because the expression in Eq. 7 is not valid for $k = 0$.

B. Imperfect detector resolution

In this section, the mass distributions are smeared out with three resolutions, 3 GeV, 6 GeV and 10 GeV, for the phase angle $\delta = 180^\circ$. These distributions are shown in Fig. 5 as well as the fitting results using the explicit signal model.

To use the F2F method, we need to multiple the second term in Eq. 7 by the exponential factor $e^{-\frac{1}{2}\left(\frac{k\pi\sigma}{L}\right)^2}$ as shown in Eq. 12. The fitting results are shown in Eq. 6 and summarized in Table II. The estimated mass and width agree well with the inputs.

Because the exponential factor suppresses the high-frequency modes very heavily, only the first few modes are important. To see this point, we can investigate more terms in the Fourier series. Figure 7 shows the first 100 terms in the Fourier series for a pure signal sample

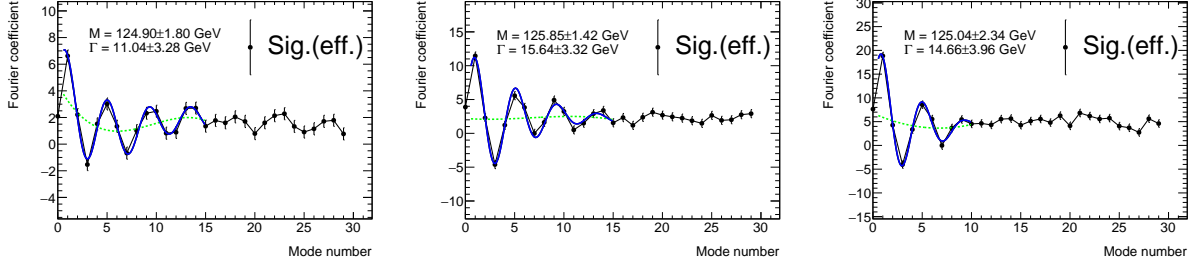


FIG. 6. (color online) Fitting results for three resolutions, 3 GeV (left), 6 GeV (middle) and 10 GeV (right). The black dots with error bar represent the Fourier coefficients of the effective signal (data subtracting background). The blue curves represent the full fitting results. The green dashed curves represents the slow-varying contribution, namely, the polynomial part in Eq. 7.

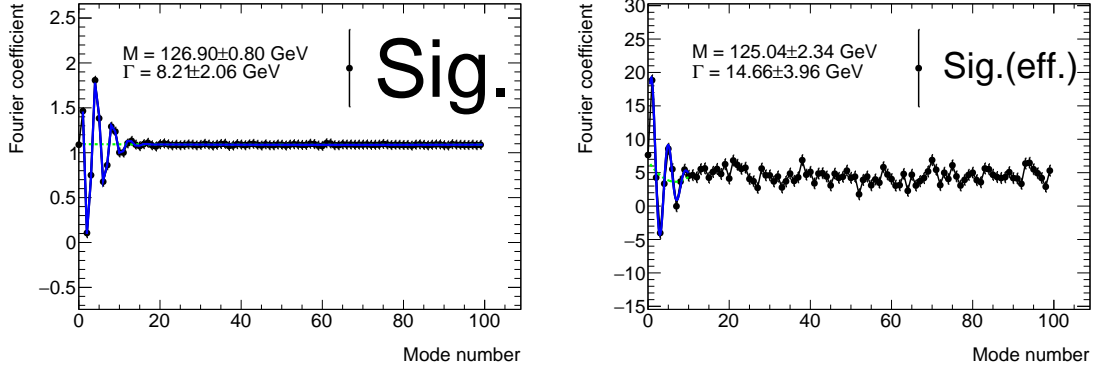


FIG. 7. (color online) Fitting results for the resolution of 10 GeV. The left plot is a fit to the pure signal sample and the right plot is a fit to the effective signal (namely data subtracting background). The black dots with error bar represent the Fourier coefficients of the effective signal (data subtracting background). The blue curves represent the full fitting results. The green dashed curves represents the slow-varying contribution, namely, the polynomial part in Eq. 7.

and for the effective signal in the case of 10 GeV resolution. Obviously, the fluctuation in the high-frequency coefficients is much smaller for the pure signal than the effective signal.

It is worth mentioning a subtle thing about smearing. By approximating a distribution function about an observable, x , by a cosine Fourier series in the range $(0, L)$, we actually assume the distribution function is symmetrical about $x = 0$ and has a period $2L$. This makes the convolution with a Gaussian function very easy to calculate as shown in Eq. 12, but also reveals a disadvantage of the Fourier series approximation. This is because the

TABLE II. Summary of the fitting results on the mass and width in the case of imperfect detector resolution.

Resolution [GeV]	Explicit signal model		F2F (this work)	
	Mass [GeV]	Width [GeV]	Mass [GeV]	Width [GeV]
3	125.17 ± 1.54	13.47 ± 3.38	124.90 ± 1.80	11.04 ± 3.28
6	126.59 ± 1.66	10.87 ± 2.77	125.85 ± 1.42	15.64 ± 3.32
10	126.02 ± 2.15	11.81 ± 3.99	125.04 ± 2.34	14.66 ± 3.96

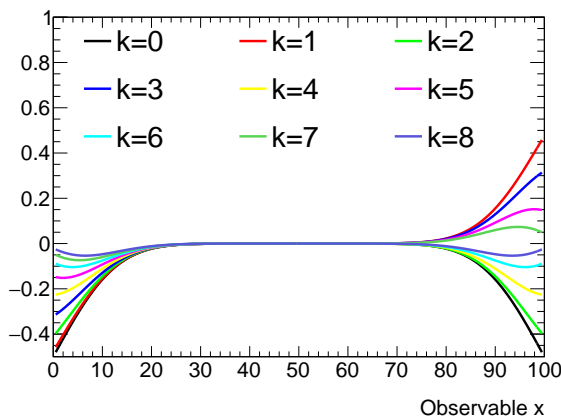


FIG. 8. (color online) The difference between the smeared distribution function with the convolution range $(-\infty, +\infty)$ and that with the convolution range $(0, 100)$ for different frequency modes. The resolution is 10.

true distribution is probably neither symmetric about $x = 0$, nor periodic. To check its potential effect, we restrict the convolution range from $(-\infty, +\infty)$ to $(0, L)$ in calculating the smeared out coefficients in Eq. 12. Supposing $L = 100$ and the resolution is 10 (the unit is non-relevant for the discussion), the smeared distribution differences between the two convolution ranges are shown in Fig. 8 for different frequency modes. As expected, the difference is only significant around the edges. Therefore we should choose a range where the structure to be studied is far from both edges by a distance of 2 times the resolution (as observed in Fig. 8).

In the end of this section, it should be emphasized that the F2F method can be also used to search for unknown particles and make statistic interpretations even if we do not observe a significant strange structure and allow potential interference.

IV. SUMMARY

The interference effect is believed to be more and more important in future searches for new particles. It is crucial to determine the mass and width of the new particle even if the interference makes the new particle show up with strange shape. In this work, a model-independent method, F2F, is proposed to search for an unknown particle and measure its mass and width when we do not have enough knowledge about the interference details. It is to perform cosine Fourier transformation to the data and background and then fit to the Fourier coefficients. The detector resolution effect can be considered conveniently. No information on the signal model is needed. Toy experiments show good agreement between the results from F2F and the inputs. The precision is only a bit worse than fitting using an explicit signal model.

V. ACKNOWLEDGEMENT

I would like to thank Fang Dai for encouraging words.

-
- [1] BESIII Collaboration, Phys. Rev. D91 (2015) 112001, arXiv:1504.03194
 - [2] ATLAS Collaboration, JHEP 1904 (2019) 048, arXiv:1902.05892
 - [3] ATLAS Collaboration, JHEP 1905 (2019) 164, arXiv:1812.07343
 - [4] CMS Collaboration, JHEP 1806 (2018) 127, Erratum: JHEP 1903 (2019) 128, arXiv:1804.01939
 - [5] CMS Collaboration, CERN-EP-2019-147, arXiv:1908.01115
 - [6] S. Jung, Y.W. Yoon, and J. Song, Phys. Rev. D93 (2016) 055035, arXiv:1510.03450
 - [7] A. Djouadi, J. Ellis, A. Popov, J. Quevillon, JHEP 1903 (2019) 119, arXiv:1901.03417
 - [8] N. Kauer, A. Lind, P. Maierhöfer, and W. Song, JHEP 1907 (2019) 108, arXiv:1905.03296
 - [9] see for example https://en.wikipedia.org/wiki/Contour_integration